Coastal uplift and tsunami effects associated to the 2010 M_w8.8 Maule earthquake in Central Chile

Gabriel Vargas[1], Marcelo Farías[1], Sébastien Carretier[2],
Andrés Tassara[3], Stéphane Baize[4], Daniel Melnick[5]

[1] *Departamento de Geología, Universidad de Chile, Plaza Ercilla 803, Santiago, Chile.*
  gvargas@ing.uchile.cl; mfarias@dgf.uchile.cl

[2] *Institut de Recherche pour le Développement, LMTG, Observatoire Midi Pyrenees, 14 av. E. Belin, 31400 Toulouse, France.*
  carretie@lmtg.obs-mip.fr

[3] *Departamento de Ciencias de la Tierra, Facultad de Ciencias Quimicas, Universidad de Concepión, Victor Lamas 1290, Barrio Universitario, Concepción, Chile.*
  andrestassara@udec.cl

[4] *BERSSIN (Seismic Hazard Division), Institut de Radioprotection et de Surete Nucleaire, IRSN BP 17, 92262 Fontenay-aux-Roses, France.*
  Stephane.Baize@irsn.fr

[5] *Universität Potsdam, Institut für Erd- und Umweltwissenschaften, Karl-Liebknecht-Str. 24-25, 14476 Potsdam-Golm, Germany.*
  melnick@geo.uni-potsdam.de

ABSTRACT. On February 27, 2010 at 03:34:08 AM an M_w8.8 earthquake, with epicenter located off Cobquecura (73.24°W; 36.29°S), severely hit Central Chile. The tsunami waves that followed this event affected the coastal regions between the cities of Valparaíso and Valdivia, with minor effects as far as Coquimbo. The earthquake occurred along the subduction of the Nazca oceanic plate beneath the South American plate. Coseismic coastal uplift was estimated through observations of bleached lithothamnioids crustose coralline algae, which were exposed after the mainshock between 34.13°S and 38.34°S, suggesting the latitudinal distribution of the earthquake rupture. The measured coastal uplift values varied between 240±20 cm at sites closer to the trench along the western coast of the Arauco peninsula and 15±10 cm at sites located farther east. A maximum value of 260±50 cm was observed at the western coast of Santa María Island, which is similar to the reported uplift associated with the 1835 earthquake at Concepción. Land subsidence values on the order of 0.5 m to 1 m evidenced a change in polarity and position of the coseismic hinge at 110-120 km from the trench. In four sites along the coast we observed a close match between coastal uplift values deduced from bleached lithothamnioids algae and GPS measurements. According to field observations tsunami heights reached *ca*. 14 m in the coastal area of the Maule Region immediately north of the epicenter, and diminished progressively northwards to 4-2 m near Valparaíso. Along the coast of Cobquecura, tsunami height values were inferior to 2-4 m. More variable tsunami heights of 6-8 m were measured at Dichato-Talcahuano and Tirúa-Puerto Saavedra, in the Biobío and Arauco regions, respectively, to the south of the epicenter. According to eyewitnesses, the tsunami reached the coast between 12 to 20 and 30 to 45 minutes in areas located closer and faraway from the earthquake rupture zone, respectively. Destructive tsunami waves arrived also between 2.5 and 4.5 hours after the mainshock, especially along the coast of the Biobío and Arauco regions. The tsunami effects were highly variable along the coast, as a result of geomorphological and bathymetric local conditions, besides potential complexities induced by the main shock.

Keywords: M_w8.8 Maule earthquake, Central Chile, Coseismic coastal uplift, Tsunami effect.

RESUMEN. Levantamiento cosísmico e impacto del tsunami a lo largo de la costa de Chile central asociado al terremoto del Maule M$_w$8,8 de 2010. El 27 de febrero de 2010 a las 03:34:08 de la madrugada un terremoto de magnitud M$_w$8,8, cuyo epicentro se ubicó costa afuera de Cobquecura (73,24°W; 36,29°S), afectó severamente la zona centro-sur de Chile. Posteriormente un tsunami afectó las costas comprendidas entre las regiones de Valdivia y Valparaíso, con efectos menores en la costa de Coquimbo. El terremoto ocurrió a lo largo de la subducción de la placa tectónica de Nazca bajo la placa Sudamericana. Se estimó el levantamiento cosísmico de la costa a partir de observaciones de la franja de algas coralina lithothamnioideas, expuesta como producto del terremoto. Evidencias de deformación vertical se observaron entre los 34,13°S y 38,34°S, sugiriendo la extensión latitudinal de la ruptura sísmica del evento principal. El levantamiento costero observado varió entre 240±20 cm, en la costa occidental de la península de Arauco, ubicada relativamente más cerca de la fosa tectónica, y 15±10 cm, en zonas más al este. En la costa occidental de la Isla Santa María se midió un valor máximo de 260±50 cm, el cual es similar a la cantidad de levantamiento cosísmico como producto del terremoto de Concepción en 1835. Subsidencia costera del orden de 0,5 m y 1 m fue estimada en áreas localizadas más al este. En términos regionales, un cambio de alzamiento a hundimiento cosísmico a lo largo de la costa ocurrió a una distancia de 110-120 km respecto de la fosa. En cuatro sitios se pudo notar una buena correlación entre valores de alzamiento cosísmico deducido a partir de la franja blanca de algas coralinas lithothamnioideas y aquel deducido a partir de mediciones geodésicas realizadas con GPS. Las mayores alturas del tsunami que afectó las costas luego del terremoto se observaron inmediatamente al norte del epicentro del sismo principal, en la Región del Maule, en donde alcanzaron hasta *ca.* 14 m, y disminuyeron progresivamente hacia el norte, hasta valores del orden de 4-2 m al sur de Valparaíso. En la costa cercana a Cobquecura éstas no superaron los 4-2 m. Alturas más variables del orden de 6-8 m se observaron en las áreas de Dichato-Talcahuano y Tirúa-Puerto Saavedra, en las regiones del Biobío y de La Araucanía, respectivamente. Los testimonios recopilados coinciden en que los tiempos de llegada del tsunami a las costas variaron desde 12-20 minutos hasta 30-45 minutos en las zonas más cercanas y más lejos de la ruptura sísmica, respectivamente. Inundaciones de tsunami afectaron las costas aún entre 2,5 y 4,5 horas después del terremoto principal, especialmente en las regiones del Biobío y de Arauco. El impacto del tsunami en la costa fue altamente variable en zonas aledañas, como producto de factores geomorfológicos y batimétricos locales, además de potenciales complejidades inducidas por la ruptura sísmica del terremoto principal.

Palabras clave: Terremoto M$_w$8,8, Chile central, Levantamiento cosísmico costero, Tsunami.

1. Introduction

On February 27th, 2010, at 03:34:08 local time (UTC -0300), a strong earthquake hit the coast of central Chile. The earthquake occurred along the subduction plate boundary between Nazca and South America, whose convergence occurs at 6.8 cm/year (DeMets *et al*., 1994; Ruegg *et al*., 2009). According to the Seismological Service of the University of Chile, the epicenter was localized at 73.24°W and 36.29°S, at 43 km offshore and SW from Cobquecura. The hypocenter was determined at 30 km depth and the calculated moment magnitude (M$_w$) was 8.8 (www.sismologia.cl; Fig. 1). The along-strike rupture length was initially estimated to be around 500 km, extending from the O'Higgins Region (Punta Topocalma; 34.14°S) to the southern part of the Arauco peninsula in the Araucanía Region (Mocha Island; 38.41°S), and severely affected the Maule region of central Chile (Madariaga *et al*., 2010; Farías *et al*., 2010; Fig. 1).

The earthquake's rupture zone covered a region previously characterized as a mature seismic gap (Ruegg *et al*., 2009), localized mainly between Constitución and Concepción (35°-37°S; Ruegg *et al*., 2009; Fig. 1). According to the historical reports of Charles Darwin and Captain Robert Fitz Roy during their reconnaissance of the Chilean coast on board the R/V Beagle, the last major subduction earthquake in this area occurred on 1835, with an estimated magnitude of *ca.* 8.5 (Lomnitz, 1971; Beck *et al*., 1998). This event caused important coseismic uplift of the Arauco peninsula (up to 3 m at the Santa María Island) as well as large tsunami waves that affected the coast of the Biobío region (Fitz Roy, 1836; Darwin, 1840, 1846). During the 20th century, previous seismic events were the 1928 Talca earthquake, which ruptured a smaller portion along the plate boundary (Lomnitz, 1971; Beck *et al*., 1998; Fig. 1), and the destructive 1939 Chillán earthquake which has been interpreted as a deeper intra-plate event (Campos and Kausel, 1990; Beck *et al*., 1998). Thus, the Maule earthquake of February
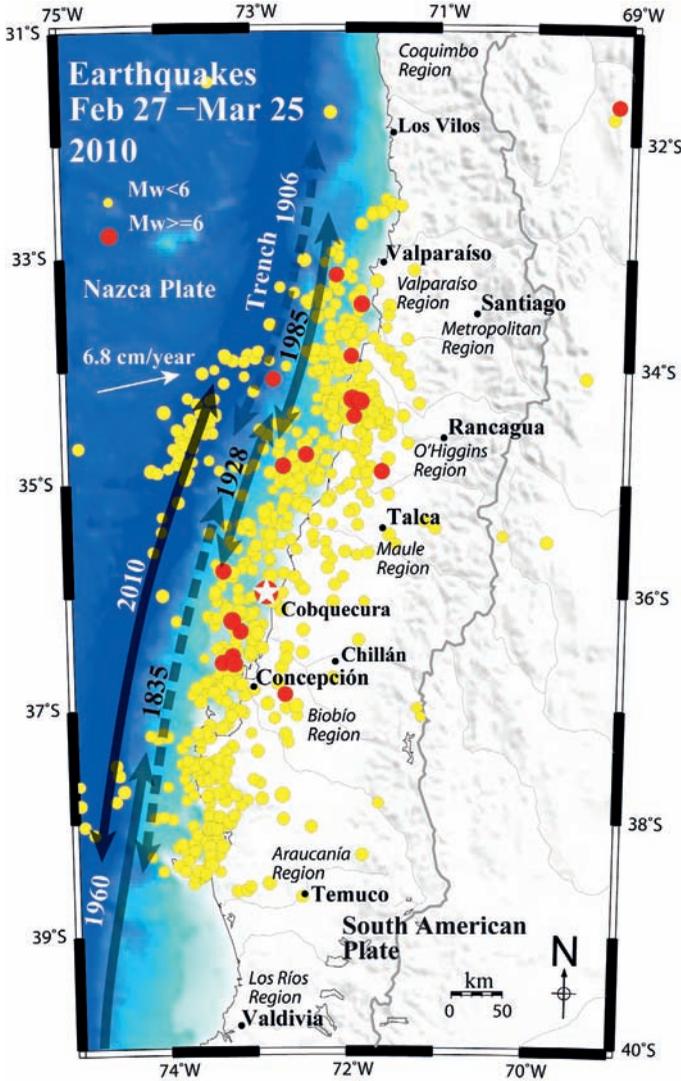
FIG. 1. Location of the epicenter of the M_w8.8 earthquake on February 27th 2010 (white star in red circle), and of the aftershocks occurred until March 25th, 2010 (US Geological Service, USGS; Seismological Service from University of Chile). The latitudinal extents of rupture zones of the earthquakes of 1835, 1906, 1928, 1960 and 1985 are also shown (Lomnitz, 1971; Beck *et al.*, 1998; Plafker and Savage, 1970; Cifuentes, 1989; Gutenberg and Richter, 1954; Comte *et al.*, 1986; Christensen and Ruff, 1986; Monfret and Romanowicz, 1986; Choy and Dewey 1988; Barrientos, 1988). Tectonic plates convergence vector according Ruegg *et al.* (2009).

27, 2010 ruptured an area which included a segment previously identified as a seismic gap. The 2010 event limited to the south with the rupture zone of the giant 1960 Valdivia earthquake (M_w9.5; Plafker and Savage, 1970; Kanamori, 1977; Cifuentes, 1989; Fig. 1), and to the north overlapped with the Valparaíso earthquakes of 1906 (M_w8.6; Gutenberg y Richter, 1954; Comte *et al.*, 1986; Fig. 1) and 1985 (M_w7.8; Christensen and Ruff, 1986; Monfret and Romanowicz, 1986; Choy and Dewey, 1988; Barrientos, 1988; Fig. 1).

The magnitude of the 2010 Maule earthquake was close to expected on the basis of modeling GPS velocities in the previously defined seismic

gap region of south-central Chile (Barrientos, 1994; Ruegg *et al.*, 2009). Based on stochastic modeling of spatiotemporal patterns of historical earthquakes, Barrientos (1994) considered a high probability (41%, 63%) for the occurrence of a great earthquake between 34.3°S and 37.2°S with an estimated maximum magnitude of M_w8.4 occurring in the year 2005±10. Based on GPS measurements obtained between 1996 and 2002, Ruegg *et al.* (2009) estimated that the southern part of the plate interface along the so-called Constitución-Concepción seismic gap had already accumulated enough strain to produce an M_w8.0-8.5 earthquake.

Few minutes after the Maule earthquake, large tsunami waves affected the coast between Valparaíso and Valdivia (Fig. 1), and strongly impacted the region between Pichilemu (34.39°S; O´Higgins Region) and Puerto Saavedra (38.81°S; Araucanía Region). The earthquake and tsunami caused 486 fatalities in addition to 79 missing persons according to official reports (www.interior.gov.cl; April 2010). In addition, the event caused substantial losses of infrastructure in areas close to the epicenter (*ca.* USD 30,000 millions, according to the Chilean Government; March 2010). In this region, horizontal Peak Ground Acceleration (PGA) of up to 6 m/s^2 were recorded (up to *ca.* 60%g; Madariaga *et al.*, 2010).

In this paper, we report measurements and describe methodological aspects related to the assessment of vertical coseismic displacements observed along the coast of central Chile during March 2010. We expand the data set presented in a recent publication (Farías *et al.*, 2010) and we include measurements of tsunami heights between Quintay (33.2°S; Valparaíso Region) and Niebla (39.8°S; Valdivia region), together with some observations concerning its effects on the infrastructure as well as on coastal erosion and deposition processes. Thus, the aim of this work is to provide a regional view of the effects of the earthquake and tsunami on the coastal region of south-central Chile.

2. Coastal Uplift and Tsunami Heights Measurements

We based our quantitative measurements of coseismic coastal uplift on coralline algae biomarkers. These estimates were complemented with qualitative observations of belt-forming algae and mollusks representative of the intertidal and shallow subtidal zones, together with the observation of coastal infrastructure and geomorphic features.

Since the pioneer use of biomarkers to estimate coastal uplift in 1835 by Captain Fitz Roy and Charles Darwin (Fitz Roy, 1836; Darwin, 1840; 1846), intertidal and subtidal algae and mollusks have been broadly used to quantify coseismic uplift (Plafker, 1964; Johansen, 1971; Lebednik, 1973; Bodin and Klinger, 1986; Castilla, 1988; Ortlieb *et al.*, 1996). Due to the variability that most of these communities exhibit in terms of their exposure to waves, and considering regional and local variations with respect to their vertical distribution in the tidal

zone, precise estimates of associated uncertainties is tenuous (Stephenson and Stephenson, 1972; Castilla, 1988; Ortlieb *et al.*, 1996).

We estimated coseismic coastal uplift values associated to the Maule earthquake by measuring the width of the white fringe resulting from exposed lithothamnioids crustose coralline algae. These organisms are widely present in coastal regions of the Pacific Ocean from the poles to the equator (Littler, 1972). These algae can be found attached to the rocks between the subtidal and the lower intertidal zones. The taxonomy of these algae is complex and precludes a rapid determination of genus or species in the field (Meneses, 1993; Castilla *et al.*, 2010). The most obvious lithothamnioids algae recognizable in the field are of reddish/pinkish color (Guiler, 1959) and turn white when suddenly exposed to solar radiation with no permanent humidification, possibly because of calcareous secretions (*e.g.,* Ortlieb *et al.*, 1996). Along the coast of central and northern Chile, these algae are abundant and can be found in different types of rocky substratum (Guiler, 1959; Stephenson and Stephenson, 1972; Meneses, 1986, 1993). As a biomarker of rapid tectonic changes along the coast, the measurement of the belt of bleached coralline algae has been used to estimate coseismic uplift associated to the 1995 Antofagasta earthquake of M$_w$8.0 in northern Chile (Ortlieb *et al.*, 1996) and also to measure the coseismic uplift associated to earthquakes in southwestern Pacific (Pelletier *et al.*, 2000; Lagabrielle *et al.*, 2003).

Following the methodology described by Ortlieb *et al.* (1996), we measured the difference in elevation between the upper limit of the white fringe of the crustose coralline algae, corresponding to the former upper limit of its distribution, prior to the earthquake, and the upper limit of the same algae in its reddish/pinkish state, corresponding to the highest vertical distribution of the living algae after the seismic event (Fig. 2). This difference was taken as an estimate of the coseismic uplift associated to the M$_w$8.8 earthquake. Through this methodology we obtained direct and locally-representative estimates of coastal coseismic uplift along the entire rupture zone. In this paper, we focus on detailed methodological aspects of this technique and expand a previous dataset (Farías *et al.*, 2010).

Error assessment of uplift measurements varies according local conditions. In the case of the observations made in rocky areas protected from the
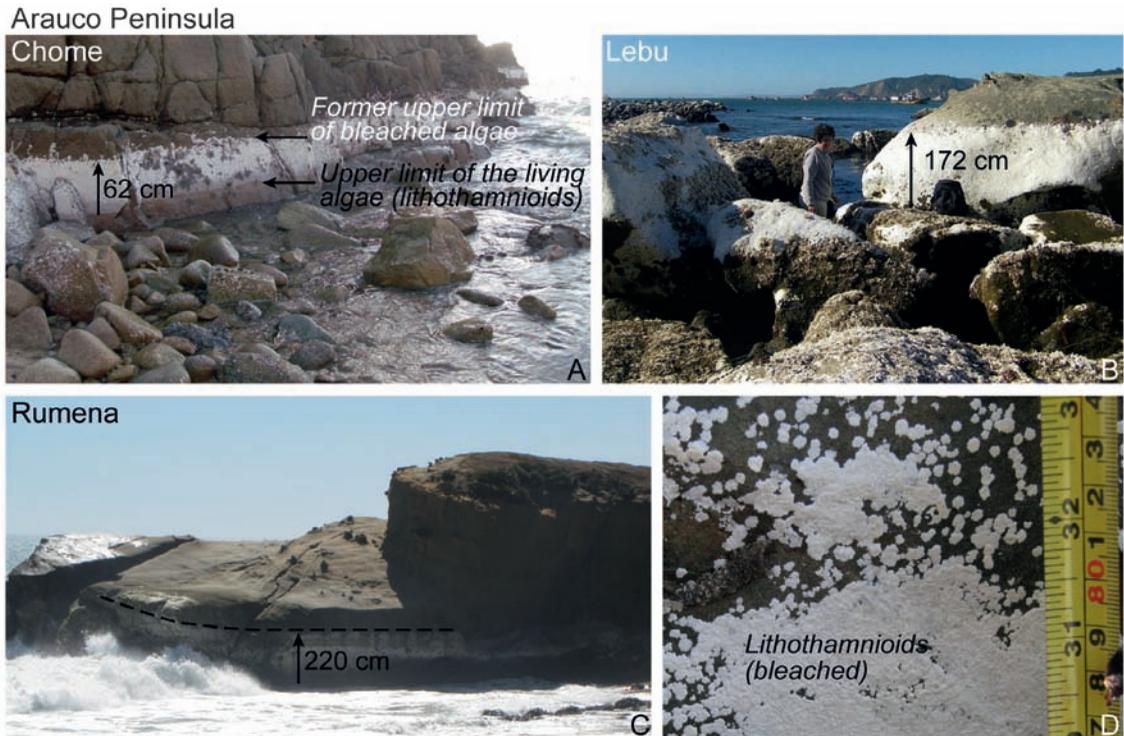
FIG. 2. Bleached lithothamnioids coralline algae strip used as a marker of coastal coseismic uplifting. **A.**, **B**. Pink (living) algae strip and white fringe of the crustose coralline algae observed at Chome and Lebu, respectively; **C**. White fringe of bleached algae at Rumena, showing increased width in the zone directly exposed to the waves; **D**. Detail of bleached lithothamnioids algae as a result of coastal coseismic uplift during the 2010 Maule earthquake.

direct influence of the storm waves, where the limits of the pre- and post-earthquake crustose coralline algae were almost horizontal, we estimated errors between ±10 cm and ±20 cm (Fig. 2). These errors were associated to the width of the band characterizing the transition from the living to the bleached algae, or by the spatial definition of the upper limit of the white fringe. At four sites (Piure, Rumena, Santa María Island and the northern extremity of Punta Lavapié), the measurements were made in areas of great exposure to waves. In those sites we observed large white fringes as the result of both coseismic uplift but also higher wave activity (Fig. 2). In addition, the direct measurement of the difference in vertical distribution between the former and the present upper limits of the algae was difficult in some areas. To take these effects into consideration, larger errors between ±20 cm and ±60 cm, estimated from the observed maximum and minimum heights of the white fringe at a given site were assumed. Thus at such sites, the errors encompass the maximum possible

width increment observed in areas directly exposed to the wave activity, between 40 cm (±20 cm) and 120 cm (±60 cm), which is similar to the amount of local increment due to the same phenomena reported by Ortlieb *et al*. (1996) from Mejillones peninsula.

Evidences of subsidence were observed on the basis of anthropogenic and geomorphologic markers in coastal and estuarine areas. Due to the difficulty to quantify the amount of subsidence in most of these sites, we present qualitative estimates and assigned conservative errors of ±40 cm and ±50 cm, which represent between 40% and 100% of the total estimates. These estimates are based on the observation of submerged terminations of river banks or estuarine terraces, flooded vegetation, submerged trees or piers, and could be partially influenced by compaction phenomena occurred during the earthquake or by erosion processes associated to the tsunami. In spite of that, we report land subsidence estimates from areas where this phenomena affected vast zones.

Local measurements of tsunami heights were conducted in areas directly exposed to the open ocean (Sugawara *et al*., 2008). We observed the highest pervasive marks left by vegetation razed by the tsunami, traces of erosion on the beach and supralittoral zones, sand and boulder deposits, and destruction provoked by the tsunami (Fig. 3). These measurements were made using a barometric altimeter with 1-m precision or with tape in sea cliffs. In order to estimate tsunami heights with respect to the sea level at the moment of its occurrence, the measurements were corrected by the tide effect according to tidal heights reported by the Navy Hydrographic and Oceanographic Service (Servicio Hidrográfico y Oceanográfico de la Armada, SHOA, Table 1). The precision for these local measurements was 1 m and therefore we assumed an error of ±0.5 m for those observations.

Thus, from field observations made between the 5th and 27th of March, our data set provides a regional view regarding coseismic vertical displacements associated with the Maule earthquake and tsunami heights along the coast located between Valparaíso and Valdivia (33.2-39.8ºS), the most severely impacted region by those phenomena (Table 2).

3. Results and Discussion

3.1. Coesismic coastal uplift and subsidence

The results of the measurements of vertical displacements along the coast with respect to their latitudinal distribution are shown in figure 4a and reported in table 2. Vertical displacements were observed between Punta Topocalma (34.14°S) and Tirúa (38.34°S). The greatest coseismic uplift was measured in the Arauco peninsula, where values reached between 133±20 cm (Yane) and 240±40 cm (Piure). Along the western coast of this peninsula, we observed large areas of exposed marine abrasion platforms resulting from coastal uplift during the Maule earthquake, with remains of intertidal algae and mollusk (Fig. 5a, e). As a result of uplift, in some areas the coastline experienced a retreat of several hundreds of meters (max. 500 m; Fig. 5b). According to our observations, the coastal area of Lebu experienced coseismic uplifting of 172±10 cm, which caused an abrupt relative descent of the sea level and consequently an abrupt drop in base level of the Lebu River, resulting in desiccation of its channel and some river banks and fluvial terraces (Fig. 5c, d). A similar phenomenon was observed in several estuaries along the western shore of the Arauco peninsula.

Measurements of the upper limit of the bleached lithothamnioids algae with respect to the local tide level at the western coast of the Santa María Island, realized in a rocky coast exposed to the direct influence of wave activity and to the open ocean, evidenced highest coastal uplift of 260±50 cm, which is on the order of the coseismic uplift of 2.4 to 3.0 m reported by the pioneer work of Fitz Roy (1836) and Darwin (1840, 1846) after the 1835 earthquake. Lower coastal uplift measurements (between 15±10 cm and 50±10 cm) were observed in small peninsulas located between Punta Topocalma (34.1°S)
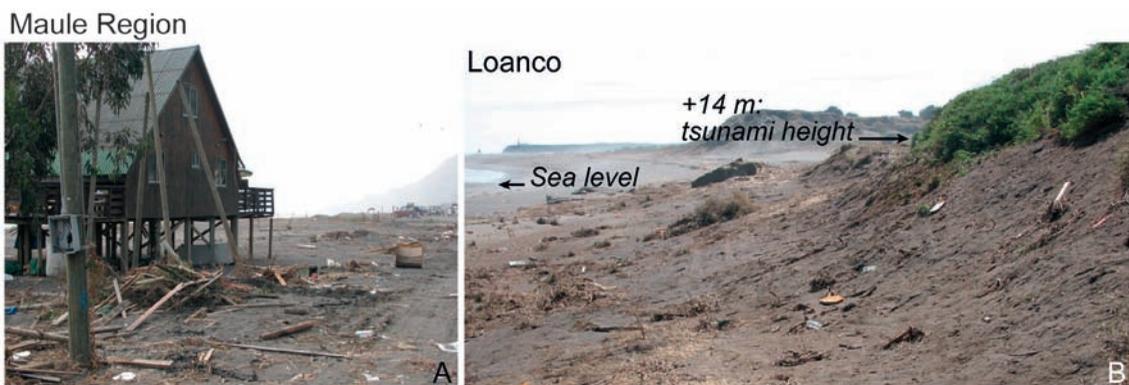
**FIG. 3.** Strong tsunami effects along the coast of Maule region. **A**. Littoral zone impacted by tsunami inundation; **B**. Marks of destroyed vegetation evidencing local tsunami height at Loanco, located northward from the epicenter of the mainshock.

TABLE 1.   HOURLY TIDAL VARIATION AS EXPECTED FROM MODEL RESULTS FOR SOME LOCALITIES IN CENTRAL CHILE AT THE MOMENT OF THE OCCURRENCE OF THE TSUNAMI OF FEBRUARY 27ᵀᴴ 2010, ACCORDING TO SHOA (WWW.SHOA.CL). B: LOW TIDE; P: HIGH TIDE.

Locality	February 26th		February 27th			
	Time	Height (m)	Time	Height (m)	Time	Height (m)
Valparaíso	21:52	1,76P	04:32	0,19B	10:24	1,33P
Talcahuano	22:17	1,83P	04:53	0,21B	10:48	1,38P
Bahía Corral	22:51	1,87P	05:30	0,18B	11:25	1,39P

and Punta Tumbes (36.6°S), along the coast of the O´Higgins, Maule and Biobío regions in south-central Chile (Fig. 1), northward from the Arauco peninsula (Fig. 4a). Uplift of similar magnitude was measured at Tirúa (38.3°S; <50 cm) and Mocha Island (38.4°S; <50 cm) located south of this peninsula (Fig. 4a), from the observation of bleached and desiccated fringes of algae and other organisms typical of the intertidal zone. From the observation of rocky shore communities, Castilla *et al*. (2010) assessed the massive mortality of belt-forming intertidal and subtidal species, such as lithothamnioids coralline algae, brown kelp and mussels, produced by the coastal uplift and tsunami that followed the Maule earthquake, estimating uplift values of 2.1-3.1 m at Santa María Island, 1.6 m at Punta Lavapié and 0.2-0.3 m at Caleta Tumbes and Mocha Island, which are similar to our estimates (Table 2).

Evidences for coseismic land subsidence were observed in places located some kilometers inland from the coastline (Figs. 6 and 7a). These observations comprise submerged quays and piers and flooded beaches, as in Bucalemu (34.6°S), flooded river bars with submerged and flooded trees and swampy vegetation, as along the Llico (34.8°S; Fig. 6a) and Biobío rivers (37°S), and possibly, submerged quays in lakes located close to the coast as the Vichuquén lake (Fig. 6b), and submerged littoral sand bars as in the case of the Mataquito river. The amount of land subsidence was roughly estimated to range between 50 cm and 1 m.

Along the coastal regions between Matanzas (33.9°S) and Quintay (33.2°S) we didn't observe detectable land level changes, neither between Puerto Saavedra (38.8°S) and Niebla (39.8°S) (Figs. 4a and 7a). This support the notion that the seismic rupture associated with the main shock of the earthquake occurred on 27 February 2010 was distributed along the 500-km-long region between Punta Topocalma (34.14°S) and Tirúa (38.34°S; Farías *et al*., 2010), as also suggested through GPS results (Vigny *et al*., 2010; Socquet *et al*., 2010).

Our estimates of vertical coseismic displacements associated to the Maule earthquake from bleached coralline algae, are consistent with uplift estimated from campaign GPS data in the same region reported by Vigny *et al*. (2010). The GPS monuments were surveyed three times before the earthquake, in 1996, 1999, and 2002, allowing the determination of stable inter-seismic velocities (Ruegg *et al*., 2009). The monuments were re-occupied immediately after the earthquake in March 2010. Co-seismic displacements were estimated by comparing the pre-earthquake position of the monuments determined by extrapolation of the 1996-2002 interseismic velocity, with the post-earthquake position. The vertical positions obtained by GPS measurements usually have an instrumental error of the order of 1 cm. In addition, the 1996-2002 interseismic rate has a standard uncertainty of 5 mm/yr, and thus its extrapolation to 2010 results in around 4 cm of error, for the site position immediately before the earthquake. Therefore most vertical co-seismic displacements measured by campaign GPS have an uncertainty of 4-5 cm (Vigny *et al*., 2010). The comparison between GPS data and our land-level measurements at the same localities (6 in total) agree within uncertainties (Fig. 8). This comparison suggests that uplift values measured from the width of the bleached lithothamnioids algae tend to underestimate the GPS coseismic coastal uplift, probably due to the uncertainty associated to the effect of high waves at sites exposed to the open ocean (Fig. 2c).

From a regional point of view, higher coseismic coastal uplifting occurred in areas closer to the trench, whereas coastal regions located eastwards experienced

TABLE 2. FIELD DATA ON TSUNAMI HEIGHT AND LAND-LEVEL VALUES ASSOCIATED TO THE 2010 MW8.8 MAULE EARTHQUAKE.

Site #	Long (°W)	Lat (°S)	Dist. To trench (km)	Locality	Obs. Local Time	Tsunami Height-Observation	Tsunami arrival time after mainshock (min)	Obs. Tsu. Height (m)	Correct. Tsunami Height (m)	(***) Add. Corr. (m)	Observed land-level change	Land-level change (cm)	Error (cm)
1	-71.700	-33.194	99.7	Caleta Quintay	17:00. Mar 09	Traces on the quay and report of witnesses.	30 min	1.5	2.2±0.6	0.22	Without apparent change.	0*	10*
2	-71.673	-33.364	104.1	Caleta Algarrobo	16:00. Mar 09	Traces on the quay and report of witnesses.	30 min	2	2.7±0.6	0.08	Without apparent change.	0*	10*
3	-71.704	-33.427	102.1	Pta. de Tralca	14:00. Mar 09	Relicts of seaweed and wood on the beach. Marks of erosion.	no data	<2	2.5±0.6	-0.15	Without apparent change.	0*	10*
4	-71.603	-33.543	112.7	Playa Grande Cartagena	13:15. Mar 09	Sand over the road and marks on the quay. Report of witnesses.	no data	2	2.4±0.6	-0.19	Without apparent change.	0*	10*
5	-71.620	-33.552	111.2	Cartagena. c. del Pirata	12:35. Mar 09	Grass and other vegetation razed by wave impact.	no data	<3	3.5±0.5	-0.19	Without apparent change.	0*	10*
6	-71.626	-33.606	111.3	Llolleo. lagoon	10:30. Mar 09	Vegetation razed over dunes. Traces of erosion by wave impact. Houses destroyed and flooded lagoon.	no data	5	5.6±0.5	-0.1	Lithothammoids not observed.	no data	no data
7	-71.634	-33.627	110.9	Rocas Santo Domingo	11:45. Mar 09	Vegetation razed over dunes. Traces of erosion by wave impact on the beach. Report of witnesses.	no data	5	5.5±0.5	-0.17	Without apparent change.	0*	10*
8	-71.845	-33.911	no data	La Boca. coast	16:30. Mar 05	Razed vegetation. Traces of erosion by wave impact on the beach and sea cliff. Report of witnesses.	no data	5	6.1±0.5	0.46	Lithothammoids not observed.	no data	no data
9	-71.844	-33.923	no data	La Boca. quay	17:30. Mar 05	Vegetation razed along river bank and fluvial terrace. Trace on the quay and report of witnesses.	no data	3	3.8±0.5	0.24	Lithothammoids not observed.	no data	no data
10	-71.879	-33.962	no data	Matanzas	19:15. Mar 05	Marks of vegetation razed on the supralittoral zone and on the river bank. Traces of wave impact on the road and houses. Report of witnesses.	no data	5	5.6±0.5	-0.19	Lithothammoids not observed.	no data	no data
28	-72.009	-34.136	92.6	Punta Topocalma	12:30. Mar 12	Razed vegetation. Traces of erosion by wave impact on the beach and supralittoral zone.	no data	9	9.4±0.5	0.00	Width of bleached Lithothamnium in a rocky coast protected from direct influence of wave activity.	40*	10*
11	-72.026	-34.393	103.3	Pichilemu	10:00. Mar 06	Houses and other constructions destroyed. Sand on the road. Vegetation razed and traces of erosion. Report of witnesses.	20-30 min	8	8.3±0.5	-0.35	Width of bleached lithothamnoids in a rocky coast protected from direct influence of wave activity.	20*	10*
12	-72.046	-34.640	122.2	Bucalemu	12:45. Mar 06	Traces on houses. Houses destroyed on the supralittoral zone. Traces of erosion by waves.	no data	8	8.6±0.5	0.14	Coastline advanced inland. Higher sea level in local harbor. Report of witnesses.	-50*	50*

Table 2 continued.

Site #	Long (°W)	Lat (°S)	Dist. To trench (km)	Locality	Obs. Local Time	Tsunami Height-Observation	Tsunami arrival time after mainshock (min)	Obs. Tsu. Height (m)	Correct. Tsunami Height (m)	(***) Add. Corr. (m)	Observed land-level change	Land-level change (cm)	Error (cm)
13	-72.037	-34.693	125.5	Puente Boyecura	14:00. Mar 06	no data	no data	no data	no data	no data	Flooded estuary bank with flooded vegetation.	-50*	50*
14	-72.061	-34.775	127.5	Puente Llico	14:30. Mar 06	no data	no data	no data	no data	no data	Flooded estuary bank with flooded vegetation.	-50*	50*
16	-72.145	-34.831	no data	Lipimavida	16:00. Mar 06	Razed vegetation. Traces of erosion on the beach.	no data	8	9.1±0.5	0.55	Possible subsidence; submerged seaweed.	no data	no data
15	-72.058	-34.844	no data	Lago Vichuquén	15:00. Mar 06	no data	no data	no data	no data	no data	Possible subsidence; flooded quay and shore lake. Higher lake level. Report of witnesses.	no data	no data
17	-72.165	-34.886	no data	Duao	17:20. Mar 06	Traces on quays. Houses and other constructions destroyed. Report of witnesses (3 waves; the first one from the SW as a "wall").	12-15 min	8	9.0±0.5	0.44	no data	no data	no data
18	-72.184	-34.967	no data	La Pesca (S-Iloca)	18:15. Mar 06	Traces on quays. Houses and other constructions destroyed. Report of witnesses (the first wave was smaller than the second one; after the first backwash, the following wave caused destruction).	20 min	10	10.8±0.5	0.29	no data	no data	no data
19	-72.181	-34.982	127.9	Mataquito River	18:30. Mar 06	Traces of razed vegetation close to the cliff.	no data	11	11.8±0.5	0.24	Flooded grass along flooded shoreline by higher sea level. Littoral bar disappeared.	-50*	50*
20	-72.495	-35.469	115.9	Las Cañas	10:20. Mar 07	Razed vegetation. Constructions destroyed and traces of erosion by wave impact on the supralittoral zone.	no data	12	12.3±0.5	0.29	Width of bleached lithothamnoids in a rocky coast; protected from direct influence of wave activity.	15*	10*
21	-72.624	-35.583	108.3	Loanco	12:25. Mar 07	Razed vegetation. Constructions destroyed. Traces of erosion on the supralittoral zone. Report of witnesses.	no data	13	13.6±0.5	0.1	Width of bleached lithothamnoids in a rocky coast; protected from direct influence of wave activity.	30*	10*
22	-72.582	-35.815	no data	Pelluhue	14:45. Mar 07	Razed vegetation. Constructions destroyed and traces of erosion by wave impact on the supralittoral zone.	no data	12	12.8±0.5	0.28	no data	no data	no data
23	-72.639	-35.842	no data	Curanipe	16:00. Mar 07	Razed vegetation. Houses and constructions destroyed on the supralittoral zone.	no data	10	11.0±0.5	0.42	no data	no data	no data
24	-72.752	-35.957	no data	Tregualemu	18:30. Mar 07	Razed vegetation. Report of witnesses.	no data	8	9.0±0.5	0.40	Possible uplift (< 1m); descent of base level of the estuary.	no data	no data
25	-72.809	-36.174	no data	Taucu	19:00. Mar 07	No destruction. Absence of traces on houses or surfaces close to the beach.	no data	<4	4.9±0.5	0.35	no data	no data	no data

Table 2 continued.

Site #	Long (°W)	Lat (°S)	Dist. To trench (km)	Locality	Obs. Local Time	Tsunami Height-Observation	Tsunami arrival time after mainshock (min)	Obs. Tsu. Height (m)	Correct. Tsunami Height (m)	(***) Add. Corr. (m)	Observed land-level change	Land-level change (cm)	Error (cm)
26	-72.816	-36.216	no data	S-Cobquecura	19:30. Mar 07	No destruction. Absence of traces on houses or soil close to the beach.	no data	<3	3.9±0.5	0.28	no data	no data	no data
27	-72.886	-36.278	no data	N-Itata	20:00. Mar 07	Vegetation razed and traces on sand littoral bar.	no data	2	2.8±0.6	0.21	no data	no data	no data
29	-73.103	-36.615	108.0	Punta Tumbes	15:45. Mar 12	Razed vegetation. Traces of erosion by wave impact.	no data	7	7.3±0.5	0.40	Width of bleached lithothamnoids in a rocky coast; protected from direct influence of wave activity.	50*	10*
48	-73.184	-36.753	106.1	Ramuncho	13:50. Mar 24	no data	no data	no data	no data	no data	Width of bleached lithothamnoids in a rocky coast; protected from direct influence of wave activity.	60*	20*
47	-73.212	-36.774	104.5	Chome	11:10. Mar 05	no data	no data	no data	no data	no data	Width of bleached lithothamnoids in a rocky coast; side protected from direct influence of wave activity; 9 measurements.	62*	20*
52	-73.004	-36.979	129.4	Biobio River	18:00. Mar 24	no data	no data	no data	no data	no data	Flooded river bank with flooded vegetation and trees.	-100*	40*
53	-73.554	-37.024	84.9	Isla Santa Maria	14:25. Mar 10	no data	no data	no data	no data	no data	Upper limit of bleached lithothamnoids in a rocky coast highly exposed to wave activity; emerged abrasion platform.	250*	60*
51	-72.984	-37.119	136.0	Biobio River	17:00. Mar 24	no data	no data	no data	no data	no data	Flooded river bank with flooded vegetation and trees.	-50*	40*
50	-72.979	-37.137	137.1	Biobio River	16:30. Mar 24	no data	no data	no data	no data	no data	Flooded river bank with flooded vegetation and trees.	-50*	40*
49	-72.978	-37.139	137.3	Biobio River	16:00. Mar 24	no data	no data	no data	no data	no data	Flooded river bank with flooded vegetation and trees.	-50*	40*
46	-73.586	-37.146	85.1	Punta Lavapié-N	18:50. Mar 15	no data	no data	no data	no data	no data	Width of bleached lithothamnoids in a rocky coast exposed to wave activity; emerged abrasion platform.	136*	20*
30	-73.587	-37.149	85.1	Punta Lavapié-S	16:10. Mar 12	Razed vegetation. Traces of erosion by wave impact. Report of witnesses.	no data	4	4.3±0.6	-0.40	Width of bleached lithothamnoids in a rocky coast protected from the direct influence of wave activity; emerged abrasion platform.	130*	10*
45	-73.613	-37.174	82.9	Rumena	14:15. Mar 25	no data	no data	no data	no data	no data	Upper limit of bleached lithothamnoids in a rocky coast exposed to wave activity; emerged abrasion platform; 5 measurements.	220*	20*

Table 2 continued.

Site #	Long (°W)	Lat (°S)	Dist. To trench (km)	Locality	Obs. Local Time	Tsunami Height-Observation	Tsunami arrival time after mainshock (min)	Obs. Tsu. Height (m)	Correct. Tsunami Height (m)	(***) Add. Corr. (m)	Observed land-level change	Land-level change (cm)	Error (cm)
44	-73.656	-37.236	79.6	Piure	16:35. Mar 25	no data	no data	no data	no data	no data	Upper limit of bleached lithothamnoids in a rocky coast highly exposed to wave activity; emerged abrasion platform; 3 measurements.	240*	40*
31	-73.323	-37.238	no data	Arauco-playa	19:00. Mar 10	No destruction. Absence of traces on houses. Report of witnesses.	no data	<2	2.9±0.6	0.32	no data	no data	no data
43	-73.666	-37.371	79.5	Yane	15:00. Mar 26	no data	no data	no data	no data	no data	Upper limit of bleached lithothamnoids in a rocky coast; side protected from the direct influence of wave activity; emerged abrasion platform; 6 measurements.	133*	20*
42	-73.643	-37.580	82.9	Lebu	14:20. Mar 07	no data	no data	no data	no data	no data	Upper limit of bleached lithothamnoids in a rocky coast; side protected from the direct influence of wave activity; emerged abrasion platform; 6 measurements.	172*	10*
32	-73.666	-37.594	82.9	Lebu	17:30. Mar 15	Seaweed trapped on a dam. Reports of witnesses (the tsunami wave entered into the estuary).	no data	<3	3.2±0.6	-0.40	Width of bleached lithothamnoids in a rocky coast; side protected from the direct influence of wave activity; emerged abrasion platform.	170*	10*
41	-73.664	-37.725	82.0	Morhuilla	19:45. Mar 08	no data	no data	no data	no data	no data	Upper limit of bleached lithothamnoids in a rocky coast protected from the direct influence of wave activity; emerged abrasion platform; 6 measurements.	214*	22*
33	-73.242	-37.981	120.5	Lago Contulmo	17:30. Mar 11	no data	no data	no data	no data	no data	Submerged fence; higher lake level. Similar to winter. No rainfall occurred after the earthquake (witnesses reports).	-30*	20*
34	-73.490	-38.249	no data	Quidico	19:30. Mar 11	Houses displaced several meters. Report of witnesses.	no data	<2	3.1±0.6	0.26	no data	no data	no data
35	-73.502	-38.342	100.1	Tirúa	14:30. Mar 12	Razed vegetation in the river-mouth.	20-30 min; other waves at 07-08 AM	7	8.2±0.5	-0.25	Bleached exposed algae and shell fringe in a rocky coast protected from the direct influence of wave activity.	<50*	
54	-73.912	-38.409	65.1	Isla Mocha	08:50. Mar 21	no data	no data	no data	no data	no data	Exposed mussel shell fringe in a rocky coast protected from the direct influence of wave activity.	<50*	
36	-73.401	-38.813	128.8	Puerto Saavedra	11:00. Mar 24	Vegetation razed on supralittoral dunes. Deposition of boulders. Report of witnesses.	20-30 min; other waves at 07-08 AM	6.5	7.1±0.5	-0.19	Without apparent change.	0*	10*
37	-73.399	-38.822	no data	Boca Budi	12:20. Mar 24	Razed vegetation. Traces of erosion by wave impact. Report of witnesses.	20-30 min; other waves at 07-08 AM	6.5	7.1±0.5	-0.23	no data	no data	no data
38	-73.221	-39.395	147.9	Caleta Queule	15:45. Mar 24	Razed vegetation. Traces on destroyed quays. Report of witnesses.	25-30 min	3	3.8±0.5	0.11	Without apparent change.	0*	10*
39	-73.397	-39.674	134.5	Niebla-N	16:30. Mar 21	Traces on the quay. Report of witnesses.		2.5	3.4±0.5	0.49	Without apparent change.	0*	10*
40	-73.389	-39.876	no data	Niebla-S	17:30. Mar 21	Razed vegetation. Traces on the quay and shoreline. Report of witnesses.	45 min. other waves at 07-08 AM	2	2.9±0.6	0.35	no data	no data	no data

(*) Data reported by Farías *et al.* (2010), (***) Additional correction to refer tsunami heights to mean sea level.
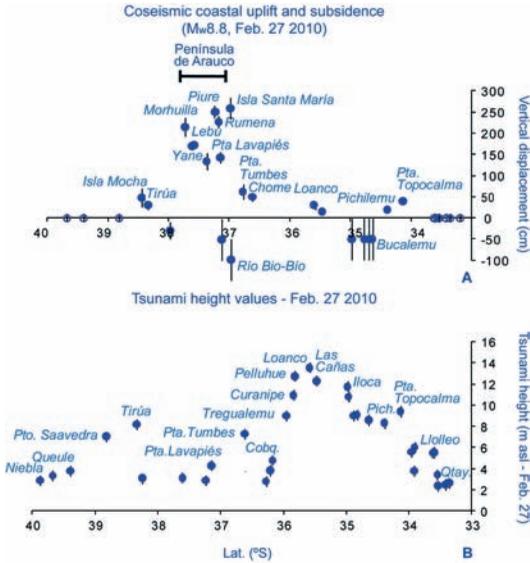
FIG. 4. Comparison of the latitudinal distribution of coseismic vertical displacements and tsunami heights along south-central Chile. **A**. Latitudinal distribution of the coastal coseismic uplift values and subsidence measurements; **B**. Tsunami height values.

lower uplift and even subsidence (Fig. 7a). A narrow hinge line for coseismic uplift/subsidence change was globally estimated at 110-120 km from the trench using the land-level changes from the entire rupture zone (Farías *et al*., 2010). Thus, the reported data are consistent with displacements mostly associated with a coseismic rebound of the continental plate, after an inter-seismic elastic deformation due to the convergence of the tectonic plates, as shown through previous GPS geodetic measurements by Ruegg *et al*. (2009) in the region. Although the slip distribution along the seismic rupture resulted from a complex process according recent model results (Socquet *et al*., 2010; Sladen *et al*., 2010; Lay *et al*., 2010; Delouis *et al*., 2010), the M$_w$8.8 Maule earthquake resulted likely from the accumulation of slip deficit along the Nazca-South American plates contact associated to their convergence at 6.8 cm/year since the last large earthquake on 1835 in south-central Chile (Ruegg *et al*., 2009; Madariaga *et al*., 2010; Farías *et al*., 2010).

3.2. Tsunami heights and coastal impact

Results from measurements of tsunami heights along the coast of central-southern Chile are shown in figures 4b and 7b. On February 27 2010, the tidal

fluctuation was the highest, among the expected variation during the period. According to a tidal model data reported by SHOA (www.shoa.cl), the tsunami that followed the Maule earthquake occurred at low tide (Table 1). Considering this fact, we corrected the tsunami height values estimated in the field, adding between +0.3 m and +1.2 m, accordingly to each locality (Table 2). Additionally, we computed the tide at the time of our measurements using the TPXO 7.1 global inverse model (Egbert and Erofeeva, 2002), and provide an additional correction to refer all our data to mean sea level.

The highest tsunami height was measured at Loanco (35.58°S; Fig. 3), which is situated immediately to the north of Pelluhue (35.84°S; Figs. 4b and 7b), in the Maule region, close to the epicenter. In fact, tsunami height values greater than 8 m were systematically observed between Punta Topocalma (34.14°S) and Tregualemu (35.96°S; Fig. 4b), along the coast of the O'Higgins and Maule regions (Fig. 1). Southwards, we observed a rapid decrease in tsunami heights, as in the coast of Cobquecura, where maximum values of 2-4 m were estimated (Fig. 4b). Farther south, tsunami height values in the order of 7 m were observed at Punta Tumbes (36.62°S; Table 2), close to Talcahuano and Dichato, which are among the most severely impacted localities by tsunami flooding. Tsunami height values around 3-4 m were observed in sites located along the western coast of the Arauco peninsula (Fig. 4b), whereas higher values were measured southwards, at Tirúa (38.34°S; 8 m) and Puerto Saavedra (38.81°S; 7 m). The observed tsunami heights diminished southwards from this locality, along the coast of the Valdivia region, up to 4 m and 3 m measured at Caleta Queule (39.40°S) and Niebla (39.67°S), respectively (Table 2). From Punta Topocalma northwards, we observed a decreasing trend in tsunami height values varying between 6 m at La Boca (33.91°S; O'Higgins Region) and 2.2 m at Quintay (33.19°S; Valparaíso Region).

The latitudinal distribution of maximum tsunami heights exhibits an irregular pattern at local scale, likely as a result of the strong control of the coastal geomorphology and bathymetry on hydrodynamics and wave splash. In fact, maximum tsunami heights were observed at coastal cliffs, whereas lower heights but larger flooded areas and greater impacts were observed in small bays and estuaries, were the tsunami caused partial or complete destruction of houses, dwellings and other infrastructure located along the supralittoral zone. Dramatic tsunami effects

Arauco Peninsula, Biobío Region

FIG. 5. Photographs showing uplifted areas along the Arauco peninsula. **A.**, **B.** Marine abrasion platform exposed at Punta Lavapié, with algae undergoing putrefaction processes, and panoramic view of a marine platform uplifted at the western coast of the Arauco peninsula, respectively; **C.**, **D.** View of the Lebu estuary with desiccated banks and river bars, resulted from the relative drop of the sea level by coastal uplifting during the Maule earthquake; **E.** Uplifted marine abrasion platform at Yane.

FIG. 6. A. Land subsidence evidenced by flooded fluvial terraces at the Llico River, and **B.** by partially submerged peers along the margin of the Vichuquén Lake, close to the coast.
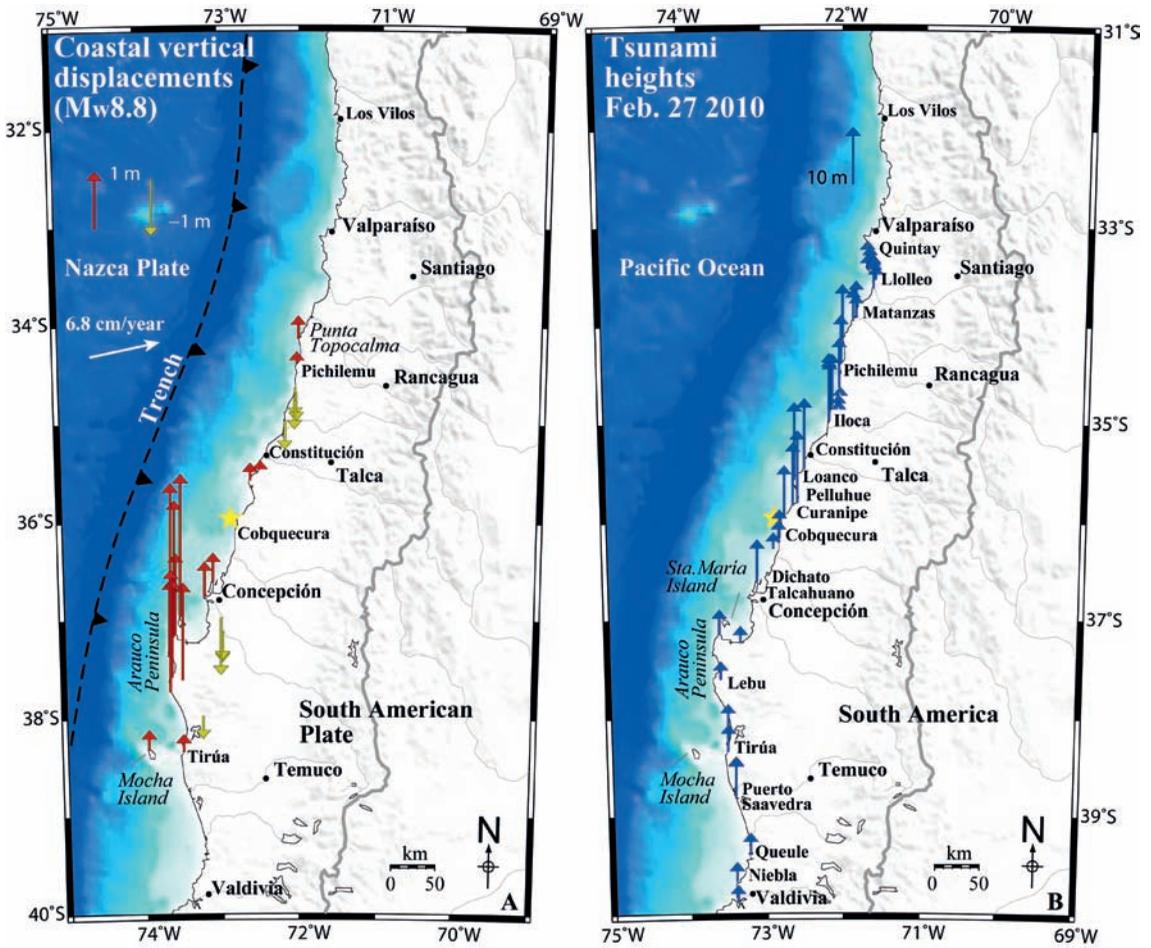
FIG. 7. A. Maps of the distribution of coastal coseismic uplift and subsidence measurements and **B.** of tsunami heights, associated with the 2010 Maule earthquake. Arrows indicate the amount of uplift (upward) or subsidence (downward) in **A.**, and tsunami height values in **B.**
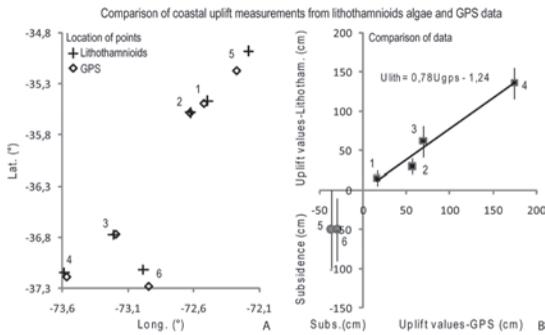
FIG. 8. Comparison of coseismic coastal uplift and subsidence estimates from lithothamnioids algae and geomorphologic markers with GPS data from Vigny *et al.* (2010). The location of sites with uplift estimates from both bleached lithothamnioids algae (crosses) and GPS measurements (diamonds) are also shown (left panel).

were observed along the coast of the Maule region, especially at Pelluhue, Curanipe and Duao-Iloca (Fig. 9), as well as at Pichilemu in the O'Higgins Region. At Dichato and Talcahuano bays, located in the Biobío region, near Concepción (Fig. 7b), the tsunami flooding reached hundreds of meters inland claiming several lives and causing serious damage to infrastructures (Fig. 10), which differ with respect to the observed reduced effects caused by tsunami inundation in some places situated just beside these localities.

Littoral bars in front of the river mouths, estuaries or lagoons, in some cases with well developed forests, appear to have protected the inner coastal areas from the direct impact of the tsunami. At Puerto Saavedra, which was highly impacted by tsunami flooding after the giant Valdivia earthquake in 1960, we observed marks of impacted vegetation and eroded supralittoral dunes evidencing tsunami heights of 7 m at the western coast of the littoral bar that protects the embayment from the direct influence of the open ocean. Contrarily to what occurred in 1960, when the town experienced strong tsunami inundations that flooded the littoral bar, the 2010 tsunami height reached 2-3 m at the inner coast of the embayment protected by this geomorphologic feature, resulting in an almost null impact on the population and local infrastructure (Fig. 11a, b, c). Similarly, while sand dunes and reinforced harbor infrastructure located on the supralittoral zone of the beach at Llolleo, in the Valparaiso region, protected the lagoon situated at the northern extremity of this area, the southern

lagoon was strongly impacted by tsunami waves that arrived from the south, which reached heights of up to 5.5 m resulting in a total destruction of modest dwellings (Fig. 12a).

Tsunami inundations caused important littoral erosion and modified the profile of several beaches (Fig. 11c, d). At several places, the most evident sedimentary deposits associated to the tsunami were sandy-gravel layers of 1-5 cm thicknesses located on the supralittoral zone (Fig. 12b, c), in some cases several hundred of meters inland, overlying organic fine deposits in lagoons and estuaries. The 2010 deposits are similar to tsunami deposits as sand layers within peat and mud sediments in coastal environments as tidal marshes, back-barrier marshes and lagoons reported in other subduction margins (Dawson and Stewart, 2007; Peters *et al.*, 2007). Additionally, we observed increased frequency of boulders in the intertidal and supralittoral zones at the western coast of the littoral bar at Puerto Saavedra, with respect to the situation before the tsunami, according to witnesses reports (Fig. 11c). The latter is comparable to the presence of large boulders left in intertidal and suppralittoral zones by historic tsunamis in other coastal areas as summarized by Dawson and Stewart (2007). These deposits resulted from onshore transport of material during run-up, analogue to present and past examples (Dawson and Stewart, 2007).

During the field survey, several eyewitnesses were interviewed and we selected only those with internal coherence in a given group of persons (N=11 cases). According to these reports, tsunami waves started to impact the coast between 12 and 20 minutes after the mainshock in areas close to the seismic rupture, as in the coastal zones located just north of the epicenter. In areas located outside the rutpure, as in the coast of Quintay and Niebla, in the Valparaíso and Valdivia regions, respectively (Table 2), tsunami waves started to arrive up to 30-45 minutes after the mainshock. According these reports, the fastest arrival of tsunami waves at the coast occurred at Loanco, situated just north of the epicenter. Model results which suggest that most of the coseismic slip associated to the mainshock occurred offshore of the area situated between the northern portion of the Biobío Region and the Maule Region, as well as offshore of the O'Higgins Region (Socquet *et al.*, 2010; Sladen *et al.*, 2010; Delouis *et al.*, 2010; Lay *et al.*, 2010), are consistent with the latitudinal distribution of coastal coseismic uplift, tsunami heights and arrival time of tsunami waves

FIG. 9. Photographs evidencing strong tsunami impact along the coast of Maule Region. **A**., **B**. Littoral area affected by tsunami inundation at Pelluhue and Duao-lloca, respectively; **C**. Tsunami impact at Curanipe, evidencing a strong effect of erosion processes on foundations of coastal infrastructure.

FIG. 10. Photograph showing dramatic tsunami impact at Dichato, along the coast of the Biobío Region.

Puerto Saavedra, Araucanía Region
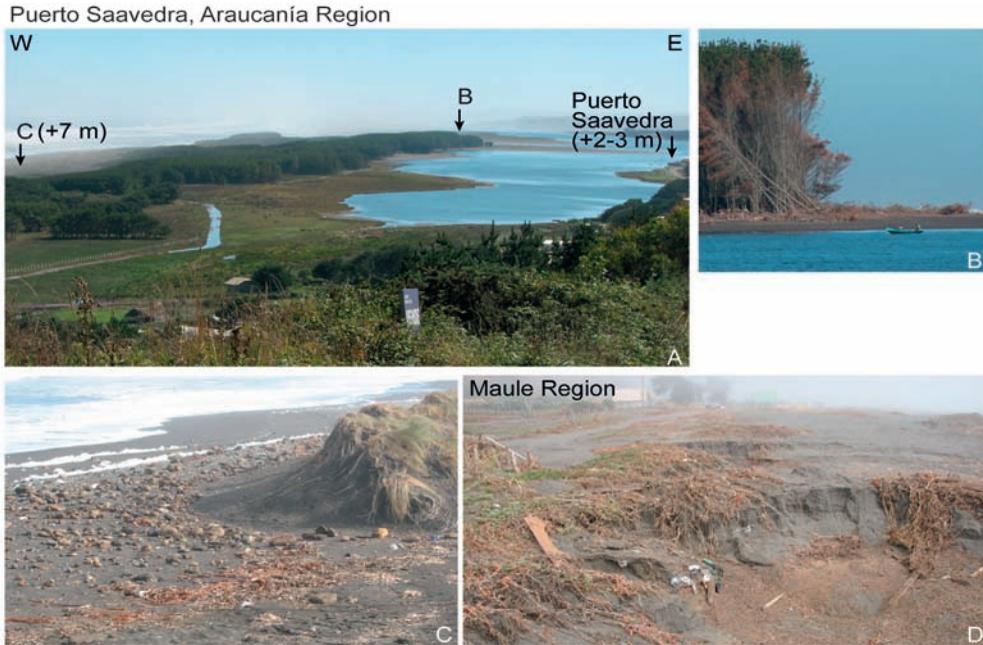
FIG. 11. A. Littoral bar covered by **B.** forest, which protects the inlet of Puerto Saavedra from the direct influence of the open ocean. **C**. The western coast of the littoral bar and possibly the woods that cover this geomorphologic feature, behaved as a dam which helped to prevent the direct tsunami impact on the coast of this locality, as evidenced by higher and lower tsunami height values observed at its western and eastern coasts, respectively. Increased accumulation of boulders on the supralittoral zone resulted from the run-up of tsunami waves at the western coast of the littoral bar, according to witnesses report. **D**. Erosion on the supralittoral zone caused by the tsunami.

FIG. 12. A. Strong tsunami impact on dwellings at Llolleo, in Valparaíso region. In this area we observed centimeters thick sandy deposits resulted from the run-up of the tsunami overlying organic and fine sediments along the margin of the lagoon. **B**., **C**. Sandy and organic rests disposed by tsunami waves on the supralittoral zone along the coast of Matanzas.

at the coast reported herein. Some witnesses coincided in three major tsunami waves, which reached the coast at periods of minutes to dozens of minutes between each other. In spite of that, some reports describe the occurrence of renewed tsunami waves at the coast of Biobío and Araucanía regions again between 06 and 08 AM local time (UTC -0300), *i.e.* 2.5-4.5 hours after the mainshock (Table 2). Additionally, eyewitness reports from Loanco, in the Maule region, indicated the arrival of tsunami waves first from the south and after from the north, suggesting a complex pattern in the occurrence of this phenomena. This is consistent with the complex bilateral rupture mode suggested by the analysis of seismic waves (Lay *et al.*, 2010).

4. Conclusions

Coseismic coastal uplift associated to the M_w 8.8 Maule earthquake of February 27, 2010 was estimated along central Chile on the basis of emerged white fringes of lithothamnioids crustose coralline algae. This method had been used successfully in other subduction earthquakes around the Pacific Ocean. The associated errors range from some centimeters up to several decimeters, and mostly depend on: (**i**) the regularity of the upper and (**ii**) lower limits of the white fringe, as well as (**iii**) the degree of exposure to strong wave activity. Our observations confirmed that the latter is the most important source of error; in areas directly exposed to the open ocean, the observed increment varied between 40 cm and 120 cm. In areas protected from the direct influence of the waves, the error can be less than 10 cm, and thus protected sites should be preferred to measure coseismic uplift. The close match between some uplift values deduced from bleached lithothamnioids with campaign GPS data, support the use of this method for a rapid reconnaissance of seismic ruptures in coastal areas.

Evidence of vertical deformation was observed between Punta Topocalma (34.14°S) and Tirúa (38.34°S), which have been considered as the maximal along-strike extent of the seismic rupture of February 27, 2010. The observed coastal uplift ranged from 15 ±10 cm to 250±60 cm, with higher values along the coast of the Arauco peninsula and Santa María Island. Uplift decreased systematically landward from the trench shifting to subsidence at an averaged distance of 110-120 km from this feature.

Largest tsunami heights, referred to the tides at the moment of the earthquake, were systematically observed in areas located immediately north of the epicenter, as along the coast of Loanco (35.58°S)-Pelluhue (35.86°S), where the tsunami reached up to 14 m. These values decreased progressively northward to 2.5 m south of Valparaíso. In turn, along the coast of Cobquecura, located in front of the epicenter of the mainshock, tsunami heights diminished to 4-2 m. A greater variability in tsunami heights was observed in the Dichato-Talcahuano area and Tirúa-Puerto Saavedra, with values around 6-8 m. Eyewitnesses reported that tsunami waves impacted the coast between 12-20 minutes after the mainshock along the Maule, Biobío and O'Higgins regions, while it reached the coast up to 30-45 minutes after the mainshock in more distant areas such as the coastal regions of Valdivia and Valparaíso. Tsunami flooding strongly affected the coast 2.5-4.5 hours after the mainshock in the Bio-Bio and Araucanía regions. The tsunami impact was highly variable at local scale, as a result of the local geomorphology and bathymetry of the coast and continental shelf, as well as from the main direction of tsunami wave propagation.

The seismic rupture occurred along the tectonic convergence of the Nazca and South American plates and ruptured an area previously characterized as a mature seismic gap, since the predecessor event in 1835. The appropriate generation and consideration of scientific knowledge in Earth Sciences is crucial to prevent the potential impact of large earthquakes in Chile, in particular, and in Andean societies, in general.

provided assistance during field trips. We thank useful comments from the reviewers J.C. Castilla, M. Cisternas and M. Pritchard, as well as from the associate editor J. Cembrano and from the editor M. Suárez. We really appreciate the useful information about the earthquake and tsunami provided by many persons during the fieldtrip realized along the coast of south-central Chile.

References

Barrientos, S. 1988. Slip distribution of the 1985 central Chile earthquake. Tectonophysics 145: 225-241.

Barrientos, S.E. 1994. Large events, seismic gaps, and stress diffusion in central Chile. *In* Tectonics of the southern central Andes (Reutter, K.J.; Scheuber, E.; Wigger, P.; editors) Springer Verlag.

Beck, S.; Barrientos, S.; Kausel, E.; Reyes, M. 1998. Source characteristics of historic earthquakes along the central Chile subduction zone. Journal of South American Earth Sciences 11: 115-129.

Bodin, P.; Klinger, T. 1986. Coastal uplift and mortality of intertidal organisms caused by the September 1985 Mexico earthquakes. Science 233: 1071-1073.

Castilla, J.C. 1988. Earthquake-caused coastal uplift and its effects on rocky intertidal kelp communities. Science 242: 440-443.

Castilla, J.C.; Manríquez, P.; Camaño, A. 2010. Effects of rocky shore coseismic uplift and the 2010 Chilean mega-earthquake on intertidal biomarker species. Marine Ecology Progress Series 418: 17-23.

Campos, J.; Kausel, E. 1990. The large 1939 intraplate earthquake of Southern Chile. Seismological Research Letters 61 (1): p. 43.

Choy, G.; Dewey, J. 1988. Rupture process of an extended sequence: teleseismic analysis of the Chilean earthquake of March 3, 1985. Journal of Geophysical Research 93: 1103-1118.

Cifuentes, I.L. 1989. The 1960 Chilean earthquake. Journal of Geophysical Research 94: 665-680.

Comte, D.; Eisenberg, A.; Lorca, E.; Pardo, M.; Ponce, L.; Saragoni, R.; Singh, S.K.; Suárez, G. 1986. The 1985 central Chile earthquake: a repeat of previous great earthquake in the region? Science 233: 449-453.

Christensen, D.G.; Ruff, L.J. 1986. Rupture process of the March 3, 1985 Chilean earthquake. Geophysical Research Letters 13: 721-724.

Darwin, C. 1840. On the connexion of certain volcanic phenomena in South America; and on the formation of mountain chains and volcanoes, as the effect of the same power by which continents are elevated.

Transactions of the Geological Society of London, 2 (5, pt.3): 601-631.

Darwin, C.R. 1846. Geological observations on South America. Being the third part of the geology of the voyage of the Beagle, under the command of Capt. Fitzroy, R.N. during the years 1832 to 1836. Smith Elder and Co. London.

Delouis, B.; Nocquet, J.M.; Vallée, M. 2010. Slip distribution of the February 27, 2010 M_w=8.8 Maule earthquake, central Chile, from static and high-rate GPS, InSAR, and broadband teleseismic data. Geophysical Research Letters 37, L17305. DOI:10.1029/2010GL043899.

DeMets, C.; Gordon, R.G.; Argus, D.F.; Stein, S. 1994. Effect of the recent revisions to the geomagnetic reversal time scale on estimates of current plate motions. Geophysical Research Letters 21: 2191-2194.

Dawson, A.; Stewart, I. 2007. Tsunami deposits in the geological record. Sedimentary Geology 200: 166-183.

Egbert, G.D.; Erofeeva, S.Y. 2002. Efficient inverse modeling of barotropic ocean tides. Journal of Atmospheric and Oceanic Technology 19: 183-204.

Farías, M.; Vargas, G.; Tassara, A.; Carretier, S.; Baize, S.; Melnick, D.; Bataille, K. 2010. Land-Level Changes Produced by the M_w 8.8 2010 Chilean Earthquake. Science 329 (5994): 916. DOI: 10.1126/ Science.1192094.

Fitz Roy, R. 1836. Sketch of the surveying voyages of his Majesty's Ship Adventure and Beagle, 1825-1836. Journal of Geological Society of London 6: 311-343.

Guiler, E.R. 1959. Intertidal belt-forming species on the rocky coasts of Northern Chile. Papers and Proceedings of the Royal Society of Tasmania 93: 33-57.

Gutenberg, B.; Richter, C.F. 1954. Seismicity of the earth and associated phenomena. Princeton University Press, 2nd edition: 310 p. Princeton.

Johansen, H.W. 1971. Effects of elevation changes in benthic algae in Prince Willian Sound. *In* The Great Alaska Earthquake of 1964. National Academy of Sciences: 35-68. Washington D.C.

Kanamori, H. 1977. The energy release in great earthquakes. Journal of Geophysical Research 82: 2981-2987.

Lagabrielle, Y.; Pelletier, B.; Cabioch, G.; Régnier, M.; Calmant, S. 2003. Coseismic and long-term vertical displacement due to back arc shortening, central Vanuatu: Offshore and onshore data following the M_w7.5, 26 November 1999 Ambrym earthquake. Journal of Geophysical Research 108 (B11): 2519, DOI:10.1029/2002JB002083.

Lay, T.; Ammon, C.J.; Kanamori, H.; Koper, K.D.; Sufri, O.; Hutko, A. R. 2010. Teleseismic inversion for

rupture process of the 27 February 2010 Chile (M$_w$8.8) earthquake Geophysical Research Letters 37, L13301. DOI:10.1029/2010GL043379.

Lebednik, P.A. 1973. Ecological effects of intertidal uplifting from nuclear testing. Marine Biology 20: 197-207.

Littler, M.M. 1972. The crustose Corallinaceae. Oceanography and Marine Biology 10: 103-120.

Lomnitz, C. 1971. Grandes terremotos y tsunamis en Chile durante el período 1535-1955. Revista Geofísica Panamericana 1: 151-178.

Madariaga, R.; Métois, M.; Vigny, Ch.; Campos, J. 2010. Central Chile finally breaks. Science 9 (328): 181-182.

Monfret, T.; Romanowicz, B. 1986. Importance of on scale observation of first arriving Rayleigh wave trains for source studies: example of the Chilean event of March 3, 1985, observed in the GEOSCOPE and IDA networks. Geophysical Research Letters 13: 1015-1018.

Meneses, I. 1986. Estado actual del conocimiento de las algas coralinaceas crustosas. Gayana Botanica 43: 19-46.

Meneses, I. 1993. Vertical distribution of coralline algae in the rocky intertidal of northern Chile. Hydrobiología 260/261: 121-129.

Ortlieb, L.; Barrientos S.; Guzmán, N. 1996. Coseismic coastal uplift and coralline algae record in northern Chile: the 1995 Antofagasta earthquake case. Quaternary Science Reviews 15: 949-960.

Pelletier, B.; Régnier, M.; Calmant, S.; Pillet, R.; Cabioch, G.; Lagabrielle, Y.; Bore, J.-M.; Caminade, J-P.; Lebellegard, P.; Cristopher, I.; Temakon, S. 2000. Le séisme d'Ambrym-Pentecôte (Vanuatu) du 26 novembre 1999 (Mw7,5): données préliminaires sur la séismicité, le tsunami et les déplacements associés. Comptes Rendus de l'Académie des sciences de Paris, Sciences de la Terre et des planètes/Earth and Planetary Sciences 331: 21-28.

Peters, R.; Jaffe, B.; Gelfenbaum, G. 2007. Distribution and sedimentary characteristics of tsunami deposits along the Cascadia margin of western North America. Sedimentary Geology 200: 372-386.

Plafker, G. 1964. Tectonic deformation associated with the 1964 Alaskan earthquake. Science 148: 1675 p.

Plafker, G.; Savage, J.C. 1970. Mechanism of the Chilean earthquake of May 21 and 22 1960. Geological Society of America Bulletin 81: 1001-1030.

Ruegg, J.C.; Rudloff, A.; Vigny, C.; Madariaga, R.; de Chabaliera, J.B.; Campos, J.; Kausel, E.; Barrientos, S.; Dimitrov, D. 2009. Interseismic strain accumulation measured by GPS in the seismic gap between Constitución and Concepción in Chile. Physics of the Earth and Planetary Interiors 175: 78-85.

Sladen, A.; Simons, M.; Bevis, M.G.; Brooks, B.A.; Foster, J.; Smalley, J.; Lin, Y.; Fielding, E.; Ortega, F.; Owen, S.; Helmberger, D.V.; Wei, Sh.; Parra, H.; Baez, J. 2010. A coseismic distributed slip model for the 2010 M$_w$8.8 Maule (Chile) earthquake. Giant earthquakes and their tsunamis, AGU Chapman Conference, Abstract Volume 47.

Socquet, A.; Bejar, M.; Vigny, Ch.; Doin, M.-P.; Ducret, G.; Carrizo, D.; Métois, M.; Peltzer, G. 2010. Modelling the source of the Maule M$_w$8.8 earthquake and early afterslip using GPS and InSAR data. Giant earthquakes and their tsunamis, AGU Chapman Conference, Abstract Volume: 48-49.

Stephenson, T.A.; Stephenson, A. 1972. Life Between Tide Marks on Rocky Shores. Freeman, W.H. and Company, San Francisco.

Sugawara, D.; Minoura, K.; Imamura, F. 2008. Tsunamis and tsunami sedimentology. *In* Tsunamiites (T. Shiki, Y. Tsuji, T. Yamazaki and K. Minoura; editors). Elsevier: 9-49.

Vigny, Ch.; Socquet, A.; Campos, J.; Carrizo, D.; Ruegg, J.-C.; Métois, M.; Sylvain, M.; Aranda, C. 2010. The Maule M$_w$8.8 earthquake monitored by continuous and survey mode GPS. Giant earthquakes and their tsunamis, American Geophysical Union Chapman Conference, Abstract: 51-52.